Indian Journal of Chemical Technology
Vol. 30, July 2023, pp. 570-578
DOI: 10.56042/ijct.v30i4.69328

Studies on characteristics and corrosion behaviour of chitosan/eudragit RS100 bilayer film coated Ti-6Al-4V

K Shreevani[1], B Narayana[1,*], B. K. Sarojini[2], A Ganesha[3], B M Praveen[4], Bharath K Devendra[4,5], Krishnakumar G[6] & Sushmitha C H[6]

[1] Department of Studies in Chemistry, Mangalore University, Mangalagangothri 574 199, Karnataka, India

[2] Department of Studies in Industrial Chemistry, Mangalore University, Mangalagangothri 574 199, Karnataka, India

[3]Department of Mechanical and Industrial Engineering, Manipal Institute of Technology, Manipal Academy of Higher Education, Manipal 576 104, Karnataka, India

[4] Department of Chemistry, Srinivas University, Institute of Engineering and Technology, Mukka 574 146, Karnataka, India

[5] Department of Chemistry, M. S. Ramaiah College of Art, Science and Commerce, MSR Nagar, Bangalore 560 054, Karnataka, India

[6] Department of Applied Botany, Mangalore University, Mangalagangothri 574 199, Karnataka, India

*E-mail:narayanab5360@gmail.com

Received 3 December 2022; accepted 8 April 2023

In the present study, implant material Ti-6Al-4V has been coated with eudragit (EU) and chitosan (CH) polymers to enhance surface properties. The deposition of polymer coating has covered the surface cracks to a significant level and the fact has been confirmed by FE-SEM coupled with EDAX wherein the atomic percentage of Ti (99.90%) in non-coated surface has been decreased markedly to 0.42% after coating. Scratch resistance and adhesion power of bilayer coating has been increased as indicated by the higher critical loads Lc_1 (16.71 N), Lc_2 (17.56 N), Lc_3 (17.96 N) when a progressive load of 1 N to 20 N is applied over the coated surface. Further, Electrochemical impedance spectroscopy (EIS) and potentiodynamic-polarization studies have shown that the value of polarization resistance is inversely proportional to the corrosion rate. Thus decrease in the corrosion rate from 107.5×10^{-2} (mm $year^{-1}$) for the non-coated alloy to 2.88×10^{-2} (mm $year^{-1}$) for CH/EU coating demonstrated that coating enhanced the corrosion resistance of the alloy in the physiological condition. The *in vitro* antibacterial test conducted against *S. aureus, B. subtilis, P. vulgaris and P. auregenosa* has shown a significant inhibition zone of 9 mm, 6 mm, 7 mm and 10 mm, respectively, thus indicating the possible application of the polymeric coating material on the dental implants.

Keywords: Dental implant, Artificial saliva, Scratch test, Potentiodynamic polarization, Critical load

Titanium and its alloys are typically employed in dental implants since they form a highly stable and protective oxide film on their surface that prevented them from being corroded in normal applications[1,2]. They are being used in dentistry devices such as implants, crowns, bridges, overdentures, and dental implant prosthesis components (screw and abutment). The Ti-6Al-4V has excellent mechanical properties and biocompatibility among different grades of titanium alloys. But it was proved that such alloys liberate titanium particles, vanadium and aluminium due to corrosion when used for the long time in biological environment[3–6]. Liberated ions have been found to be causing toxic effects which therefore should be avoided[7–11]. The implant failure could also be attributed to implant fractures, wear of the articulating surfaces, stress-shielding effect, septic or aseptic inflammation, infections on and around the implants, material fatigue, and excessive activity by the patient and debonding at the tissue-implant interface etc[12,13]. Taking everything into consideration the researchers had developed various methods to improve osseointegration, biocompatibility and surface characteristics like anti-corrosive, antibacterial and mechanical properties. One of the best methods to modify the surface is coating. Numerous coating techniques such as sol-gel, dip-coating, drop-casting, electrodeposition, plasma spraying, thermal oxidation etc have been reported for the deposition of organic/inorganic/composite coatings on implant surfaces[14,15].

It is well-known that the adhesion strength of the coating is one of the important characteristics of the coated implants in biomedical applications. Among the different methods available, scratch test is a good practice to examine the nature of adhesion strength of the coating on implant surface. This consists of

deforming the surface by indentation under the load of a moving diamond tip. Micro-indentation technique is a fairly mature technique which records depth of the scratch or penetration of an indenter into the specimen upon the application of a particular load. The original scratch depth is called as the penetration depth. Since polymers are viscoelastic materials, they should recover or heal after the scratch and this depth which is determined after the surface scratch has been finished is known as residual depth. In a material that recover well, the residual depth will typically be much less than the penetration depth[16,17]. The minimum load that damages the coating is called critical load, L_c. Higher adhesion is characterised by higher critical load.

Recently, many studies have focused on modifying the surface of an implant by biopolymer coating[6,18–20]. Chitosan is a natural polymer that is soluble in acidic conditions due to the protonation of the amine group which gives a cationic nature to the polymer. Chitosan and its derivatives possess desirable properties like biocompatibility, bioactivity, biodegradability, antibacterial property, non-toxicity and muco-adhesiveness[21]. However, pure chitosan films show poor flexibility, brittle nature and fragile behaviour[22]. Therefore its properties could be enhanced by combining it with another synthetic or natural biocompatible polymer. Polymers such as eudragit, polyethylene oxide, polylactic acid could be used for this purpose[23]. Eudragit polymers are synthetic, copolymers derived from esters of acrylic and methacrylic acids that have been used for drug delivery systems for many years[24]. Among them eudragit RS 100 [i.e., poly(ethyl acrylate, methyl-methacrylate, and chlorotrimethyl-ammoniumethyl methacrylate) co-polymer containing quaternary ammonium groups in 4.5–6.8%] is insoluble at physiological pH but soluble in organic solvents like acetone, alcohol[25].

To date, the bilayer polymer coating consisting of chitosan/eudragit RS 100 in Ti-6Al-4V is not studied much. Previously chitosan/eudragit E 100 was electrophoretically deposited on titanium grade 2 substrates by Łukasz Pawłowski et al.[26]. They found that the addition of eudragit E100 into chitosan coatings greatly decreased its degradation rate in the artificial saliva. The coating also showed higher corrosion resistance than the bare metal.

The present study aims at developing a bilayer polymer coating of chitosan/eudragit RS100 through a simple spread-casting method on Ti-6Al-4V (titanium grade 5). It is well known that one of the important facts regarding the coating is its adhesion to the substrate as well as its surface characteristics. Therefore the study focuses on the chemical analysis of the coated samples by various characterization techniques and investigation of their mechanical, anti-corrosive and antibacterial properties.

Experimental Section

Materials

Titanium alloy of grade 5 (Ti-6Al-4V) was selected as a substrate. 90% deacetylated chitosan of medium molecular weight used in the work was purchased from Sisco Research laboratories and eudragit (Molecular weight – 32,000 g/mol) from Evonik Industries as test samples. Other chemicals used in the study include acetic acid, acetone that are procured from Merck, India. Artificial saliva solution has a composition of Na_2HPO_4 (0.26 g/L), NaCl (6.7 g/L), NaH_2PO_4 (0.20 g/L), KCl (1.20 g/L), $NaHCO_3$ (1.50 g/L), bovine albumin (0.1 g/L), sodium azide as a preservative (0.1%). Double distilled water was used in the preparation of solutions.

Preparation of metals

Titanium alloy coupons of 3×1 cm^2 were used for the various characterization techniques. The samples were sequentially abraded with SiC papers of different grit sizes ranging from 600 to 1200 grades. The polished metal substrates were then ultrasonically washed with acetone, ethanol and finally with distilled water for 10 minutes each. Thereafter the metal samples were passivated in a 1:5 (v/v) nitric acid-deionized water solution for 20 min at 40°C, rinsed with deionized water for several times. For the electrochemical corrosion studies, only 1cm^2 was exposed during the experiment.

Preparation and development of polymer coating

Chitosan was dissolved in 1% v/v acetic acid solution to prepare 1% w/v aqueous solution followed by stirring at 600 rpm at 50°C on a magnetic stirrer. The solution was filtered to obtain a clear solution. Eudragit solution was prepared by dissolving 1 g of eudragit RS 100 in acetone followed by stirring. The coating was done using a simple spread-casting method. Typically 150 µL of the solution was homogeneously spread on a 1 cm^2 area of the surface of the metal alloy using a micropipette (THERMOSCIENTIFIC, INDIA). The Ti/CH/EU

sample consists of an EU layer over a CH layer on a titanium alloy substrate. The polymer-coated metal alloy was dried in a vacuum oven at room temperature for 48 h. The chitosan, eudragit and eudragit-chitosan bilayer coatings were coded as Ti/CH, Ti/EU and Ti/CH/EU respectively.

Characterization of coating

The crystalline state of the sample was analysed using a high-resolution Rigaku 600 Miniflex benchtop X-ray diffractometer with Cu Kα radiation (λ=1.5406 nm) produced at 40 kV and 30 mA to scan the diffraction angles (2θ). Field Emission Scanning Electron Microscopy coupled with Energy Dispersive X-Ray Spectroscopy (FESEM- EDAX; Carl Zeiss, Germany) and Atomic Force Microscopy (AFM; A. P. E. Research SRL, Italy) is used to study the surface morphology and elemental composition of the coatings.

Micro-mechanical evaluation

The polished surfaces of the Ti alloy and the polymer-coated samples were indented with a Vickers diamond indenter in a standard microhardness tester MATSUZAWA (MMT x-7A) under the applied load of 100 g (0.9806 N).The samples were subjected to five trials of which average values are considered. The scratch studies were performed over the surface using the Revetest RST3 instrument for all the coated samples and then compared the results with that of non-coated alloy. A 200 μm diameter diamond indenter is used to apply a progressively increasing load from 1 N to 20 N with the scratch speed of 2 mm min^{-1} and over a length of 5 mm. The parameters measured here were penetration depth and residual depth to evaluate the performance of the coating.

Electrochemical measurements

Electrochemical studies were carried out using the CHI 608D electrochemical workstation at 30 ± 2°C. The conventional three-electrode system was used for this purpose. The titanium alloys with different polymer coatings were employed as the working electrode. Saturated calomel electrode and platinum electrode were used as reference and counter electrodes, respectively. Working electrodes of area 1 cm^2 were exposed in the electrolyte of artificial saliva solution for 400 s to attain an equilibrium potential. The Electrochemical Impedance Spectroscopic studies were carried out using 10mV perturbing AC voltage in a frequency range of 0.01 Hz to 100 kHz on the open circuit potential (OCP). The impedance data were analyzed by using a Nyquist plot. The charge transfer resistance (R_{ct}), the double-layer capacitance (C_{dl}) and other parameters were deduced from the simulation of impedance data with an equivalent circuit using ZSimpWin version 3.21 software. The potentiodynamic current-potential curves were recorded by polarizing the specimen to -0.5 V cathodically and +0.5 mV anodically with respect to OCP at a scan rate of 0.001 Vs^{-1}. The corrosion rate was obtained from the Tafel extrapolation method.

In vitro antibacterial assay

The antibacterial property of the coatings is tested against two Gram-positive bacteria *Staphylococcus auereus (S. auereus)* (MTCC 96), *Bacillussubtilis (B. subtilis)* (MTCC 441)and two Gram-negative bacteria *Proteus vulgaris* (*P. vulgaris)* (MTCC 1771), *Pseudomonas aeruginosa* (*P. auregenosa)* (MTCC 424) by disc diffusion method. For this 100 μL of suspension containing bacterial culture (10^{-5} CFU/mL) was spread uniformly on Muller Hinton agar medium. In addition to the coated metal of 1 cm^2 surface area, sterile 6 mm diameter filter paper discs impregnated with 20 μL of the test material were placed on agar medium. The non-coated alloy was taken as negative control and streptomycin (10 μg/mL) was used as a positive control. The inoculated plates were incubated at 37°C for 24 h and the zone of inhibition was measured. All the experiments were performed in triplicate.

Results and Discussion

Surface morphological analysis

The FE-SEM images of (a) bare Ti alloy, (b) CH coated Ti alloy, (c) EU coated Ti alloy and (d) CH/EU coated Ti alloy are given in Fig. 1(i). The figures indicated that the morphology of the polymer-coated samples, in general, seems to be uniform. The observed grooves in the non-coated alloy is due to the mechanical polishing[27]. The deposition of polymer coating has covered the surface cracks to a significant level and thus the surface has become smoother and crack-free. The elemental analysis of coated samples was done by energy dispersive X-ray spectroscopy (EDAX). This confirmed the presence of titanium (Ti), aluminium (Al), vanadium (V), oxygen (O), carbon (C) and nitrogen (N).The spectra along with their atomic and weight percentage on the coated

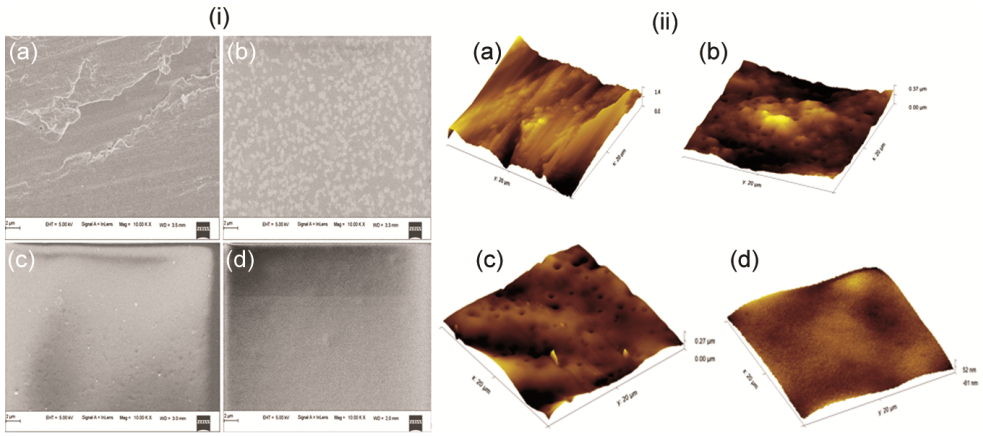

Fig. 1 (i) — FE-SEM and (ii) 3D AFM images of (a) non-coated Ti alloy, (b) Ti/CH, (c) Ti/EU and (d) Ti/CH/EU

titanium alloy is shown in the Fig. S1.The spectrum of the non-coated sample showed a 99.90 atomic percentage of titanium whereas the intensity of peak was markedly decreased in the coated samples and accordingly other constituents of the coatings (C, O and N) were increased thereby ensuring the existence of coating. Furthermore, EDAX did not show any impurities or contaminations in the coating. In the case of EU coating, Ti peak indicated a 4.80 atomic percentage which might be attributed to the lower thickness of the film-coated, as EU/acetone solution viscosity was low compared to CH/acetic acid.

The surface morphology and roughness was further analyzed by 3D images of atomic force microscopy (AFM). As shown in Fig. 1(ii) and Fig. S2 the surface of the bare alloy was found to be rougher with a surface average roughness (R_a) of 169.3 nm. As it is stated, the uniform and homogeneous morphology of the coated samples are characterized by the lower R_a values which were demonstrated herewith the values of 158.3 nm, 115.3 nm and 14.58 nm for Ti/CH, Ti/EU and Ti/CH/EU, respectively, hence complimenting the SEM images[28]. Owing to the polishing of bare titanium alloy, it showed high surface roughness which had been successfully covered by the uniform biopolymer coating and hence the roughness was decreased[28]. It was also stated that lower surface roughness was favourable for corrosion resistance due to the fact that a smoother surface has smaller potential difference[20,29].

X-ray Diffraction (XRD)

The morphology of polymer coating was further established by PXRD and the results are represented in Fig. 2. Within the obtained patterns only the peak corresponding to titanium is identified with highest

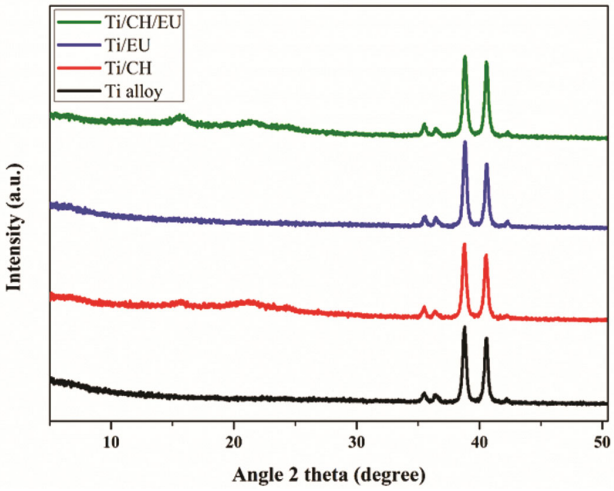

Fig. 2 — X-Ray diffraction patterns of (a) non-coated Ti alloy, (b) Ti/CH, (c) Ti/EU and (d) Ti/CH/EU

intensity that may be attributed to relatively thin polymer coating. Thus, the characteristic peaks at 35.4°, 36.4°, 38.8°, 40.5° were assigned to the nature of the alloy[30]. The semi crystalline nature of pure CH coating was indicated in the two characteristic broad peaks near 2θ =15.4° and 21°[(Ref. 31)]. The latter one could be assigned to the intramolecular and intermolecular hydrogen bonds that account for the crystallinity in chitosan[32,33]. The EU showed a negligible peak indicating its amorphous nature which was also illustrated in SEM Fig.1 (i).

Micro-mechanical study

The influence of novel polymer coating on the micro-mechanical property, scratch depth and recovery of titanium alloy has been analyzed. It is well known that hardness is an essential parameter for implants which provides information on resistance to

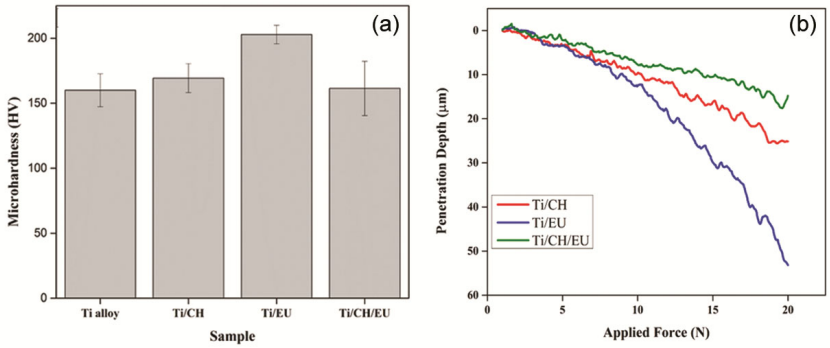

Fig. 3 (a) — Micro-hardness for different coated samples obtained with Vickers indenter (b) penetration depth for coated and uncoated titanium alloy as a function of applied load

plastic deformation under stress conditions[27]. The HV values of the developed coating on the Ti alloy is obtained by means of the Vickers microhardness test is depicted in Fig. 3(a). The values range between 162 HV and 203 HV for the coated samples. The outcome of the study revealed that the alloy with the coating exhibited higher hardness (169, 203 and 162 HV for Ti/CH, Ti/EU and Ti/CH/EU, respectively) in comparison to the bare alloy (160 HV).

The scratch depth and its recovery were evaluated as a function of the applied load in the progressive mode. The penetration depth and residual depth which was measured in microns altogether demonstrate clearly the difference in the behaviour of coated and non-coated specimens. From Fig. 3(b), it was observed that by the application of same scratch load over the same distance for all the samples resulted in the diminution in the penetration depth in comparison to the bare alloy thereby creating a resistance to applied scratch on the surface. The decrease in the scratch depth for bilayer coating than monolayer CH and EU coatings indicated that interfacial friction between the indenter tip and the material was decreased substantially[34]. Eventually, this made penetration more difficult in a dental implant if any loads were applied. Fig. S3 depicted the viscoelastic healing of the materials which was analysed by considering the recovery rate of the polymer coating[35,36]. The percentage of recovery was calculated according to the Eq. 1.

$$\% \text{ Recovery} = \frac{P_d - R_d}{P_d} \times 100 \quad \ldots (1)$$

Where P_d is penetration depth and R_d is residual depth.

The high recovery rate of the polymer bilayer coating in comparison to the individual polymer was observed during the initial stages of the scratching. As the indenter moves further there observed a similar behaviour in the CH and CH/EU coating. This might be attributed to the fact that chitosan was structurally similar to the glycosaminoglycan that facilitates the mechanical bonding between the polymer coating and the metal surface[37]. It was also evident that higher applied force provided an increase in the recovery of the coating[16]. The Fig. 4 (a-c) shows the data generated by the instrument during progressive load-scratch tests using a 200 µm radius cone indenter that relates the scratch test parameters viz. normal force, penetration depth, residual depth and scratch profile plotted as a function of the scratch length for the different samples.

The critical loads (L_c) were the loads at which different failures occur in the coating and this was the important parameter to measure the adhesion property of coatings. It is stated that L_c depends on the coating thickness, phase composition, hardness and porosity[38,39]. In general, as the scratch loading was increased three critical loads were observed. The L_{c1} corresponds to the appearance of noteworthy cracks. The L_{c2} stands for the applied normal load at which the extent of damage is increased and cohesive spallation is noted. The L_{c3} is attributed to total failure and detachment of the coating[38,40,41]. The coating was only pressed below the critical load without any damage. By comparing Fig. 4(a), (b), (c) and (d), it was obvious that as the scratch load was increased progressively and there observed a nearly-linear change in the penetration depth initially. As the critical load was reached (which is indicated in Fig. 4(a), (b), (c) by a vertical line) a notable fluctuation in the curve took place. The force values that correspond to the critical loads were indicated by the vertical line in the same figure. This was the onset of the rupture

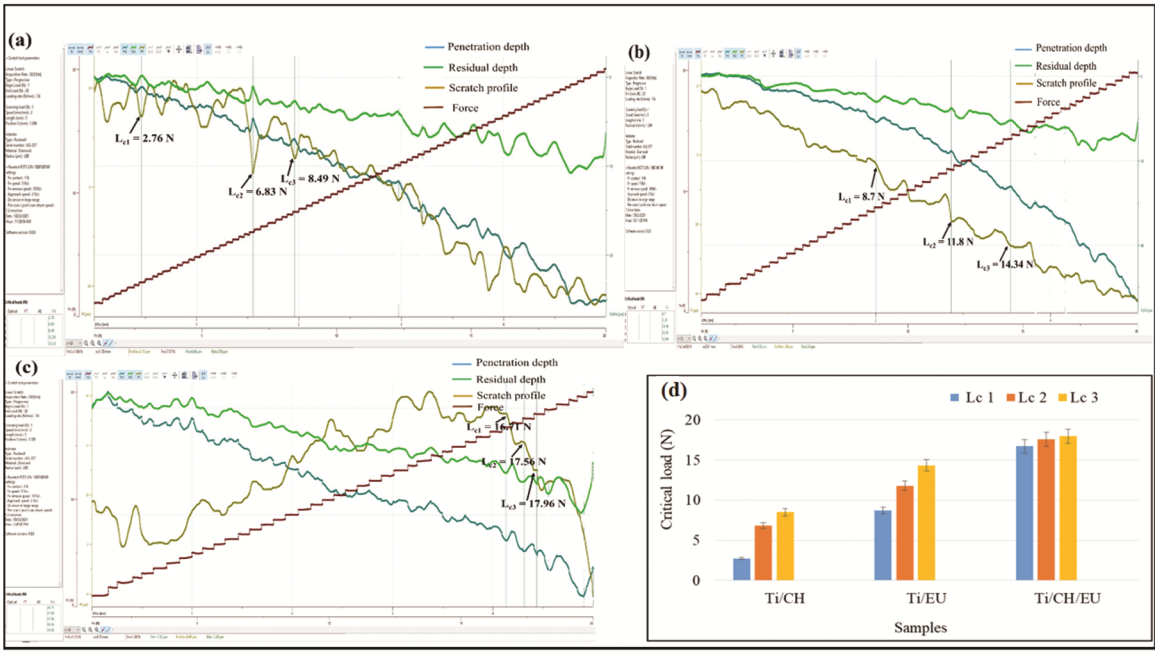

Fig. 4 — Tribological characteristics of a microscratch along the samples with penetration depth and residual depth as a function of the scratch distance (a) Ti/CH, (b) Ti/EU, (c) Ti/CH/EU and (d) Critical loads of different polymer coatings

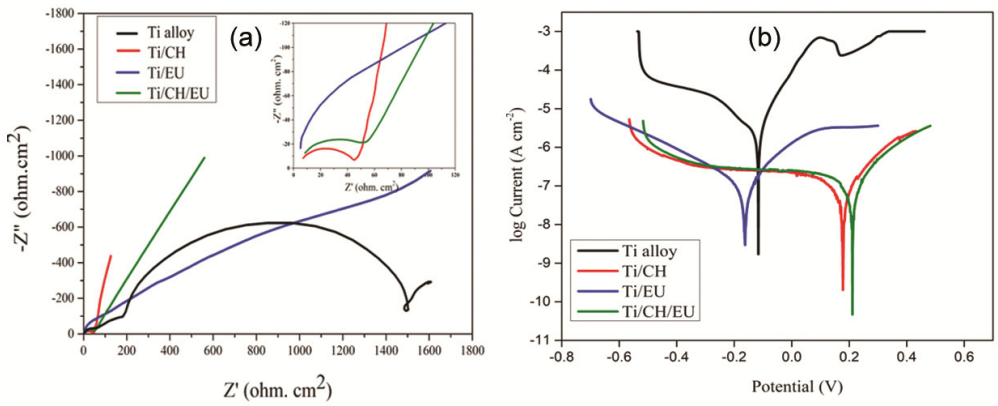

Fig. 5 (a) — Nyquist plots and (b) polarization curves for the corrosion of non-coated and polymer-coated samples

behaviour of the different coating[42,43]. The obtained L_c values for the different coated samples are summarized in Fig. 4 (d). The adhesion of chitosan on the Ti alloy surface was lower as it was indicated by the lower critical load due to its lower thickness (87 µm). In contrast, the highest adhesion was shown by the bilayer coating as it was experienced by the higher L_c. The result goes well with the fact that L_c increases with the thickness of the CH/EU coating (92.67 µm) owing to a proportional increase in its interfacial force[39]. All these inferences might be attributed to the fact that the surface becomes more strong and harder with the presence of an additional layer of EU on CH. Thus increased thickness and strong adhesion of the coating with uniform surface morphology thus enhanced the mechanical property of the implant material[26,44].

Electrochemical impedance spectroscopy (EIS)

The Nyquist plots for the non-coated and polymer coated Ti alloy are depicted in the Fig. 5(a). The plot of the bare alloy exhibits three semi-circles followed by a Warburg diffusion at the higher and low-frequency regions, respectively. These three capacitive loops could be attributed to the charge transfer process of the alloy (contains Ti, Al and V) and due to the dissolution of the natural TiO_2 layer[45].

Table 1 — Different electrochemical parameters calculated from the EIS measurements in synthetic saliva

Sample	$C_{dl} \times 10^{-6}$ (F)	R_s (Ω cm^2)	R_{ct} (Ω cm^2)	R_p (Ω cm^2)	W (Ω)	Q-$Y_0 \times 10^{-5}$ (F)	Q-n
Ti alloy	21.11	30.34	393.08	423.42	0.29	7.61	0.96
Ti/CH	0.19	61.51	804.03	865.54	2.14	5.40	0.88
Ti/EU	0.08	43.82	841.45	885.27	1.98	3.01	0.85
Ti/CH/EU	0.14	47.09	886.82	933.91	3.04	5.26	0.71

Table 2 — Polarization data for tested samples

Sample	E_{corr} (V)	$I_{corr} \times 10^{-6}$ (A cm^{-2})	Corrosion rate$\times 10^{-2}$ (mm year^{-1})	Degree of corrosion protection (%)
Ti alloy	-0.116	3.91	107.5	-
Ti/CH	0.178	0.10	4.17	96.12
Ti/EU	-0.162	0.12	3.41	96.83
Ti/CH/EU	0.211	0.15	2.88	97.32

The plots of polymer coated samples exhibit only one semicircle at the high-frequency region followed by a diffusion controlled behaviour.

It was the common knowledge that the resistance corresponds to semi-circles at the high-frequency region was the measure of resistance against the corrosion and the Warburg diffusion was the resistance against the diffusion of corrosion medium into the specimen[46]. The resistance along the real axis is determined to be higher for Ti/CH/EU and it was observed that the coated samples displayed one semi-circle in the Nyquist plot, which was due to the surface coverage of specimen by the coating disallowing the corrosion medium to interact with the specimen and thus, retarding the corrosion process. During the inhibition process of polymer-coated specimen only one type of surface was in contact with the corrosion therefore the generation of single semi-circle. The impedance behaviour obtained was simulated to an equivalent circuit as shown in the Fig. S4. The equivalent circuit consists of five elements, where R_s is the resistance offered by the solution, R_{ct} is the charge-transfer resistance, Q is the constant phase element (CPE) which corresponds to the capacitance (C) of the double layer, and W is Warburg impedance. The polarization resistance R_p calculated using the Eq. (2) are found to be inversely proportional to the corrosion rate[47]

$$R_p = R_s + R_{ct} \quad \ldots (2)$$

The values of different EIS parameters calculated from the experiment are listed in the Table. 1. As it is evident from the data, the polarization resistance R_p was found to be inversely proportional to the corrosion rate. The increased value of R_p for coated samples clearly signifies the surface resistance offered by the polymer coating thereby hindering the ion diffusion[48].

Potentiodynamic polarization method

The Tafel curves obtained are given in Fig. 5 (b) and the corrosion parameters calculated are given in the Table. 2. It could be seen from the table that the coated samples were having much lower corrosion current density (I_{corr}) and corrosion rate as compared to the bare alloy. It had been proved that higher the value of corrosion current and corrosion rate, more the metal was prone to corrosion[49]. Corrosion potential (E_{corr}) of the bare alloy in the salivary condition was found to be -0.116 V which, shifts towards the anodic side in the case of polymer coating except for EU. This significant shift in the corrosion potential and reduction in the corrosion current was due to the protective nature of the polymer film on the metal. The corrosion inhibition efficiencies were calculated using the Eq. (3)

$$IE = \frac{I_{corr*} - I_{corr}}{I_{corr*}} \times 100 \quad \ldots (3)$$

Where, I_{corr*} and I_{corr} are the current density of uncoated and coated specimens, respectively. The high values of protection efficiency of the CH, EU and EU-CH coatings on titanium alloy indicated the enhancement of corrosion resistance by the polymers.

It was well established that in neutral conditions, the anodic reaction would be the passage of metal ions into the electrolyte and the cathodic reaction would be the oxygen reduction as mentioned in Eqs (4) and (5)[50–52]

$$Ti \rightarrow Ti^{4+} + 4e^- \quad \ldots (4)$$

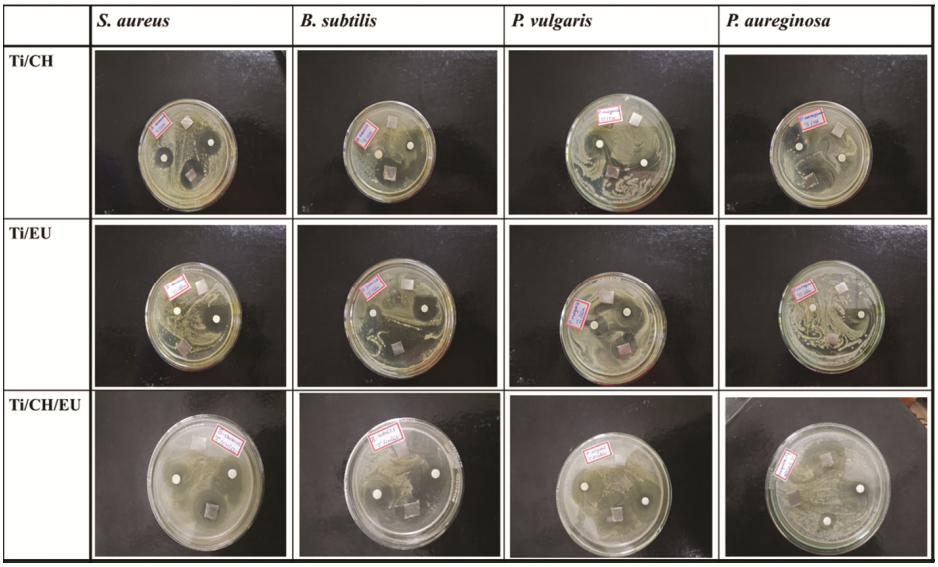

Fig. 6 — Inhibition zone of selected bacteria against polymer coated samples after 24 h of interaction

$$O_2 + 2\ H_2O + 4\ e^- \rightarrow 4\ OH^- \quad \ldots (5)$$

As the chitosan molecule is having a larger size and high molecular weight it was expected that the film could cover the metal surface to a large extent thereby forming a barrier to the corroding ion from the surrounding environment. It was also stated that the presence of nitrogen and oxygen in the CH and EU will help in the adsorption and binding of the molecule well on the surface[15,52].

Antibacterial activity

The bactericidal action of the polymer coatings obtained by the disc diffusion method is depicted in Fig. 6. Compared with bare alloy, polymer-coated samples have excellent antibacterial properties against all the tested organisms. Only Ti/EU shows no inhibition zone against *P. aureginosa*. The increase in the bactericidal activity of bilayer coated sample is indicated by the increase in the inhibition zone as depicted in the Fig. S5. It shows the maximum activity of 10 mm diameter zone against *P. aureginosa.* The antibacterial property of chitosan and eudragit RS 100 are widely investigated and they are found to be active against various bacteria like *S. aureus*, *E. coli*, *B. subtilis*[53-55]. It is obvious that chitosan and eudragit are cationic in nature due to protonated amino group. This interacts with the negatively charged microbial cell membranes and results in the local rupture of the intracellular components of the microorganism[55]. However, it was stated that the antibacterial activity of chitosan depends on molecular weight, pH of the environment and degree of deacetylation[54].

Conclusion

Herein a polymer bilayer coating of CH and EU had been prepared on Ti-6Al-4V by a simple and environmental friendly process of spread casting. The characterization results from FESEM-EDAX, AFM and XRD confirmed the homogeneous and uniform coating over the alloy surface. The effect of the coating was analyzed by comparing the corrosion rates and mechanical properties of the coated and non-coated alloy samples. Potentiodynamic polarization studies indicated that developed polymer bilayer coating was capable of acting as a good corrosion resistant in physiological conditions with an inhibition efficiency of 97.32%. Furthermore, the mechanical study provided a deep insight into the deformation and healing response of the material and nature of different failure modes. Thus the scratch test revealed that the developed coating resisted deformation and a higher critical load for the CH/EU indicated its higher load carrying capacity. The developed coatings also showed good bactericidal activity against *S. aureus* (MTCC 96), *B. subtilis*(MTCC 441), *P. vulgaris* (MTCC 1771) and *P. aureginosa* (MTCC 424). Hence, the polymer bilayer (CH/EU) coating fabricated on the alloy is found to be a promising one with enhanced physical, mechanical, anti-corrosive and antibacterial properties and could be used in dental implant materials for improving their characteristics.

Acknowledgment

The authors are thankful to KSTePS, DST, Govt. of Karnataka for providing the financial help and the coordinator of the DST-PURSE laboratory, Mangalore University for providing instrumental facilities.

Supplementary Information

Supplementary information is available in the website http://nopr.niscpr.res.in/handle/123456789.

References

1 Chen C S, Chang J H, Srimaneepong V, Wen J Y, Tung O H, Yang C H, Lin H C, Lee T H, Han Y & Huang H H, *Sur Coat Technol*, 399 (2020) 126125.
2 Yamazoe J, Nakagawa M, Matono Y, Takeuchi A & Ishikawa K, *Dent Mater J*, 26 (2007) 260.
3 Kheder W, Al K S, Khalaf K & Samsudin A R, *Jpn Dent Sci Rev*, 57 (2021) 182
4 Prestat M &Thierry D, *Acta Biomater*, 136 (2021) 72.
5 Schiff N, Dalard F, Lissac M, Morgon L & Grosgogeat B, *Eur J Orthod*, 27 (2005) 541.
6 Bosh N, Deggelmann L, Blattert C, Mozaffari H & Müller C, *Surf Coa Technol*, 347 (2018) 369.
7 Elias C N, Lima J H C, Valiev R & Meyers M A, *Biol Mater Sci*, 60 (2008) 46.
8 Hansen D C, *Electrochem Soc Interface*, 17 (2008) 31.
9 Souza J C, Henriques M, Oliveira R, Teughels W, Celis J P & Rocha L A, *Biofouling*, 26 **(**2010) 471.
10 Rodríguez-Mercado J J, Roldán-Reyes E & Altamirano-Lozano M, *Toxicol Lett*, 144 (2003) 359.
11 Domingo J L, *Neurotoxicol Teratol*, 17 (1995) 515.
12 Zhao L, Chu P K, Zhang Y & Wu Z *J*, *Biomed Mater Part B*, 91 (2009) 470.
13 Kirmanidou Y, Sidira M, Drosou M E, Bennani V, Bakopoulou A, Tsouknidas A, Michailidis N & Michalakis K, *Biomed Res Int*, 2016 (2016) 2908570.
14 Xiong D, Yang Y & Deng Y, *Surf Coat Technol*, 228 (2013) S442.
15 Hussein M S & Fekry A M, *AsCS Omega*, 4 **(**2019) 73.
16 Brostow W, Bujard B, Cassidy P E, Hagg H E & Montemartini P E, *Mater Res Innov*, 6 (2002) 7.
17 Brostow W, Deborde J, Jaklewicz M & Olszynski P, *J Mater Educ,* 24 (2003) 119.
18 Biasetto L, Elsayed H, Bonollo F & Colombo P, *Surf Coat Technol*, 301 (2016) 140.
19 Flamini D O & Saidman S B, *Corros Sci*, 52 (2010) 229.
20 Duan Y, Wu Y, Yan R, Lin M, Sun S & Ma H, *Int J Biol Macromol*, 184 (2021) 109.
21 Fakhri E, Eslami H, Maroufi P, Pakdel F, Taghizadeh S, Ganbarov K, Yousefi M, Tanomand A, Yousefi B, Mahmoudi S & Kafil H S, *Int J Biol Macromol*, 162 (2020) 956.
22 Mishra S K & Kannan S, *J Mech Behav Biomed Mater*, 40 (2014) 314.
23 Kouchak M, Handali S & Naseri B B, *Osong Public Health Res Perspect,* 6 (2015) 14.
24 Amaresh P, *Int J Pharm Sci Res*, 8 (2017) 4973.
25 Lopedota A, Trapani A, Cutrignelli A, Chiarantini L, Curci R, Manuali R & Trapani G, *Eur J Pharm Biopharm*, 72 (2009) 509.
26 Pawłowski Ł, Bartmański M, Strugała G, Mielewczyk-Gryń A, Jazdzewska M & Zieliński A, *Coatings*, 10 (2020) 607.
27 Rikhari B, Pugal M S & Rajendran N, *Carbohydr Polym*, 189 (2018) 126.
28 Ballarre J, Aydemir T, Liverani L, Roether J A, Goldmann W H & Boccaccini A R, *Surf Coat Technol*, 381 (2020) 125138.
29 Wei X, Liu P, Ma S, Li Z, Peng X, Deng R & Zhao Q, *Corros Sci*, 173 (2020) 108729.
30 Kandiah K, Duraisamy N & Ramasamy B, *J Nanobiotechnology*, 12 (2018) 211.
31 Kumar S & Koh J, *Int J Mol Sci*, 13 (2012) 6103.
32 Mahmoudzadeh M, Fassihi A, Emami J, Davies N M & Dorkoosh F, *J Drug Target*, 21 (2013) 693.
33 Ren L, Zhao Y, Yang L, Cao W, Wang H, Lian X, Gao X, Niu B & Li W, *Surf Coat Technol*, 420 (2021) 127319.
34 Sinha S K, Song T, Wan X & Tong Y, *Wear*, 266 (2009) 814.
35 Dela Isla A, Brostow W, Bujard B, Estevez M, Rogelio R J, Vargas S & Castaño V M, *Mater Res Innov*, 7 (2003) 110.
36 Sung L, Comer J, Forster A M, Hu H, Floryancic B, Brickweg L & Fernando R H, *J Coat Technol*, 5 (2008) 419.
37 Zhang J, Dai C S, Wei J & Wen Z H, *Appl Surf Sci*, 261 (2012) 276.
38 Madhan K A, Hussein M A, Adesina A Y, Ramakrishna S & Al-Aqeeli N, *RSC Adv*, 8 (2018) 19181.
39 Hariprasad S, Gowtham S, Arun S, Ashok M & Rameshbabu N, *J Alloys Compd*, 722 (2017) 698.
40 Shtansky D V, Gloushankova N A, Bashkova I A, Petrzhik M I, Sheveiko A N, Kiryukhantsev-Korneev F V, Reshetov I V, Grigoryan A S & Levashov E A, *Surf Coat Technol*, 201 **(**2006) 4111.
41 Aldrich-Smith G, Jennett N M & Housden J, *Thin Films*, 46 (2004) 1.
42 Chouanine L, Takano M, Ashihara F & Kamiya O, *J Mater Sci*, 40 **(**2005) 5703.
43 Komath M, Rajesh P, Muraleedharan C V, Varmah K, Reshmi R & Jayaraj M K, *J Mater Sci*, 34 (2011) 389.
44 Jugowiec D, Łukaszczyk A, Cieniek L, Kot M, Reczyńska K, Cholewa-Kowalska K, Pamuła E & Moskalewicz T, *Surf Coat Technol*, 319 (2017) 33.
45 Martinez A L, Brugnoni L I, Flamini D O & Saidman S B, *Prog Org Coat*, 144 **(**2020) 105650.
46 Ruhi G, Modi O P & Dhawan S K, *Synth Met*, 200 **(**2015) 24.
47 Medhashree H & Shetty A N, *J Adhes Sci Technol*, 33 (2019) 523.
48 Mogera U, Kurra N, Radhakrishnan D, Narayana C & Kulkarni G U, *Carbon*, 78 (2014) 384.
49 Kaur S, Sharma S & Bala N, *Mater Chem Phys*, 238 **(**2019) 121923.
50 Mouhyi J, Dohan E D M & Albrektsson T, *Clin Implant Dent Relat Res,* 14 (2012) 170.
51 Akbarzadeh E, Ibrahim M N M & Rahim A A, *Int J Electrochem Sci*, 6 (2011) 5396.
52 Fernández-Pérez B M, González-Guzmán J A, González S & Souto R M, *Int J Electrochem Sci*, 9 (2014) 2067.
53 Atay H Y, *Functinal Chitosan*, (Springer) (2020).
54 Akhtar M A, Mariotti C E, Conti B & Boccaccini A R, *Surf Coat Technol*, 405 **(**2021) 126657.
55 Tripathi S, Mehrotra G K & Dutta P K, *Bull Mater Sci*, 34 (2011) 29.